Journal of Engineering and Science Research 6 (5): 06-11, 2022
e-ISSN: 2289-7127

DOI: 10.26666/rmp.jesr.2022.5.2

Analysis of Multilevel Otsu Thresholding for Corrosion Rate of Anodised AZ91D Magnesium Alloy

Zuraila Iberahim[1], Mohd Zamzuri Mohammad Zain[1], Abdul Halim Ismail[2], Ng Suit Mun[3], Farah Izzati Subri[1], Nooraizedfiza Zainon[1], Elmi Abu Bakar[4]

[1]Faculty of Mechanical Engineering Technology, Universiti Malaysia Perlis, Pauh Putra Campus, 02600 Arau, Perlis, Malaysia.

[2]Faculty of Electrical Engineering Technology, Universiti Malaysia Perlis, Pauh Putra Campus, 02600 Arau, Perlis, Malaysia.

[3]Faculty of Electronic Engineering Technology, Universiti Malaysia Perlis, Pauh Putra Campus, 02600 Arau, Perlis, Malaysia.

[4]School of Aerospace Engineering, Universiti Sains Malaysia, Engineering Campus, 14300 Nibong Tebal, Pulau Pinang, Malaysia.

Received: 15 August 2022; Revised: 02 September 2022; Accepted: 05 October 2022; Published: 30 October 2022

Abstract: Magnesium and its alloy are renowned for their high strength-to-weight ratio, excellent machinability and good castability, making it a favourable material for manufacturing various automotive parts. But when exposed to the environment, magnesium and its alloy have a weak ability to resist corrosion. AZ91D magnesium alloy was anodised and immersed in a salt solution to accelerate deterioration. The image of the corroded surface resulting from the immersion test was analysed by quantising the corroded regions. This paper studies the feasibility of an image processing approach using the multilevel Otsu thresholding method by quantising the corroded region on the AZ91D magnesium alloy. This method converts the original colour image to a greyscale image and then converts it to a binary image and RGB image for the multilevel thresholding. The pixel distributions from the multilevel Otsu thresholding display a trend that, with a higher corrosion rate, the pixel's frequency of occurrence shifted more to the darker regions. This conforms with the Otsu thresholding, where the darker region is identified as the corroded area of the AZ91D magnesium alloy. By implementing the negative image, the binary image is segmented into non-corroded and corroded areas and labelled as 0 (black) and 1 (white,) respectively. As for multilevel Otsu thresholding, the RGB image is assigned in three colours representing different corrosion severity regions. The regions of the corrosion severity are categorised into severe corrosion, moderate corrosion and low corrosion, coloured in dark blue, light blue, and yellow, respectively. Thus, the trend of the corrosion activity can be seen by implementing the multilevel Otsu thresholding and correlating it with the corrosion rate value. Furthermore, obtaining data on corrosion attack severity can provide helpful information in predicting a component's failure and future maintenance planning.

Keywords: *Image processing, Corrosion, AZ91D Magnesium alloy, Quantitative assessment, Anodising, Multilevel Otsu Thresholding*

INTRODUCTION

Magnesium and its alloy are well known for their exceptionally low weight but high strength, widely used in automotive and aerospace parts manufacturing. The benefit of having a high strength-to-weight ratio, excellent machinability and good castability is unfortunately deterred by its low corrosion resistance to the environment [1].

Metals deteriorate and degrade by the chemical or electrochemical reaction when exposed corrosive

Corresponding Author: Zuraila Iberahim, Faculty of Mechanical Engineering Technology, Universiti Malaysia Perlis, Pauh Putra Campus, 02600 Arau, Perlis, Malaysia

environment [2]. Prolonged exposure can lower and eventually damage their mechanical properties and lead to catastrophic failure [3]. There are many types of corrosion depending on their environment and initiation mechanism, but uniform corrosion and pitting corrosion commonly happen on a surface. For this work, pitting corrosion is observed due to its manner of pits, small cavities or holes that penetrate deeper into the samples. To fully utilised the AZ91D magnesium alloy in automotive components fabrication, surface treatment such as conversion coating [4], laser treatment [5], anodising [7,8] and many more were usually done on the material to improve the corrosion resistance.

Corrosion analysis of a material can be evaluated through various techniques such as weight loss [8], electrical resistance monitoring [9], linear polarisation resistance [10], which requires experimental setup and the most common technique of visual inspection that requires experts. Image processing techniques shows various promising result in corrosion evaluation. One of the early applications of image processing on pitting corrosion was made by [11] for pitting probability. Then more corrosion evaluation was applied, such as detecting and differentiating corroded surface from the background surface [12] and identifying pitting corrosion from other types of corrosion [13]. Most of the previous studies were done on the uncoated sample or actual structures such as ships [14], marine structures [15], pipelines [16] and bridges [17] with different processing techniques.

This study aims to implement multilevel Otsu thresholding on the anodised and AZ91D magnesium alloy samples. The analysis of the multilevel Otsu thresholding method on the AZ91D magnesium alloy corrosion rate was investigated. The correlation between corrosion rate and total corroded pixel was also used.

METHODOLOGY

Table 1 summarised the condition of the AZ91D magnesium alloy samples used in this study. A total of eight samples were divided into groups, Group 1 and Group 2, according to the electrolyte concentration (Zinc Nitrate) used during the anodising process. From each group, only three samples will be immersed in NaCl solution for corrosion test while the remaining sample remains anodised with no further corrosion testing. This sample will act as a reference sample against the three corroded samples.

Table 1. Description of AZ91D magnesium alloy samples.

Group	Sample	Sample's Condition
	Sample 1A	Anodised (reference)
Group 1 (0.01M)	Sample 1B to 1D	Anodised and corroded
Group 2 (0.1M)	Sample 2A	Anodised (reference)
	Sample 2B to 2D	Anodised and corroded

Figure 1 shows the image processing flowchart after the corrosion image is acquired. After selecting the corroded area as the region of interest (ROI), multilevel Otsu thresholding is applied, and the pixel numbers are analysed.

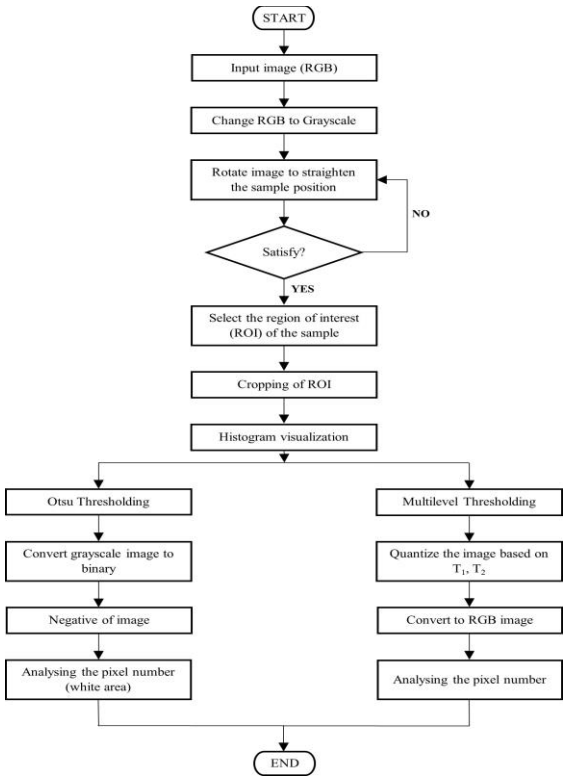

Fig. 1. Flow chart of corrosion image processing.

Sample Preparation

In this study, AZ91D magnesium alloy was used as the substrate. Its primary composition consists of nearly 90 wt% magnesium, 8.5-9.5 wt% aluminium, 0.45-0.9wt% zinc, 0.17-0.4wt% manganese and t, and the elements such as silicone, copper, ferrous, nickel is less than 0.05 wt%. Eight AZ91D magnesium alloy samples with identical sizes of 10 mm × 10 mm × 10 mm were prepared and cold mounted. All samples were polished with 1200 grit sandpaper before the anodising process.

The anodising process was conducted in a Zinc Nitrate solution with two different electrolyte concentrations of 0.01M (Group 1) and 0.1M (Group 2) for 3 minutes at 20V. After anodising, the samples were dry for 24 hours at 70 ±2°C. Afterwards, three anodised samples from each group were immersed in NaCl

solution for corrosion testing as per standard JIS H0541:2003 (Method of Alkaline Salt Corrosion Testing for Magnesium and Magnesium Alloy). The immersion was done for 72 hours at 35 ±2°C, and then the samples were cleaned and dried again for 24 hours at 70 ±2°C. The weight of the samples after each drying stage were recorded to calculate the weight loss for the corrosion rate, R in millimetre per year, using the equation below:

$$R = \frac{8.76 \times 10^4 W}{ADt} \quad (1)$$

Where W, A, D, and t are weight change (g), active area (cm^2), density (g/cm^3) and immersion time (h), respectively.

Image Acquisition

A setup of an imaging chamber occupied with LED illuminations and plain background was used to ensure a nearly uniform brightness distribution (Figure 2). Inside the imaging chamber, a base is used to place the sample in a fixed position. The device used to acquire the image, iPad Pro 11, is stationed opposite the corroded sample's surface at a 7 cm distance.

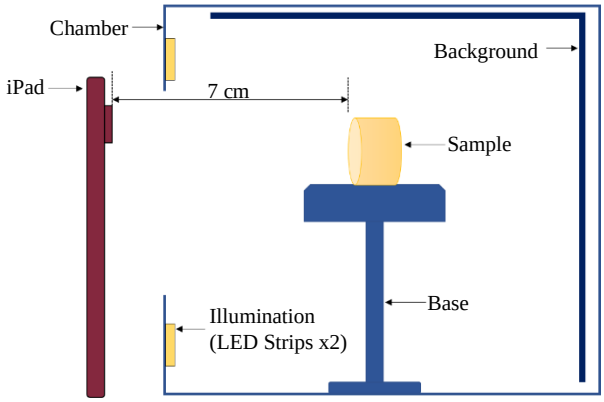

Fig. 2. Image chamber setup for corrosion image acquisition.

Table 2 shows the camera specifications for iPad Pro 11, used in the image acquisition process. The default photo setting was used without flash, and the timer was disabled. All photos were captured by pressing the shutter manually at 1x zoom.

Table 2. iPad Pro 11 camera specifications.

Display size	11.0"
Resolution	1668 × 2388 pixels (~264 PPI density)
Main Camera	Triple 12 MP (Back camera)
Magnification	2× optical zoom out Digital zoom up to 5×
Illumination	Backside illumination sensor
Mode	Photo

DETECTION OF CORROSION

Corrosion Image Input

From the input image, it was converted to grayscale and cropping was done to select the region of interest (ROI), which is the corroded surface of the AZ91D magnesium alloy sample Figure 3(a). Once the ROI has been selected, the corroded region will be cropped from the background Figure 3(b), and the histogram of each sample will be visualised.

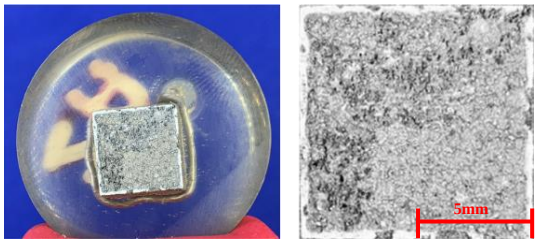

(a) (b)

Fig. 3. Raw sample image before cropping (a) and after cropping (b).

Corrosion Region Quantization

Otsu thresholding and multilevel Otsu thresholding were applied to the grayscale image to analyse the corroded region of the sample's surface. At Otsu thresholding, a negative image was implemented to the binary image and enhanced the white or grey detail embedded in the dark regions of the corroded surface [18]. The white region was then categorised as corroded and black as non-corroded areas.

Meanwhile, for multilevel Otsu thresholding, the corroded region of the image was quantised at T_1 and T_2 and then converted to an RGB image. The regions were divided into low corrosion region, moderate corrosion region, and severe corrosion region labelled as yellow, light blue and dark blue, respectively. Pixel numbers from each thresholding method were then analysed further.

RESULT AND DISCUSSION

Thresholding Image Output

Shown in Figure 4 is the example of the surface appearance of an anodised and corroded sample. For instance, in Figure 4(a), the anodised reference sample has a flat and smoother surface compared to corroded samples because the sample doesn't go through a corrosion test. Meanwhile, Figure 4(b) shows the example of a corroded sample where the irregular surface and different depths of pit holes caused by the corrosion attack can be seen.

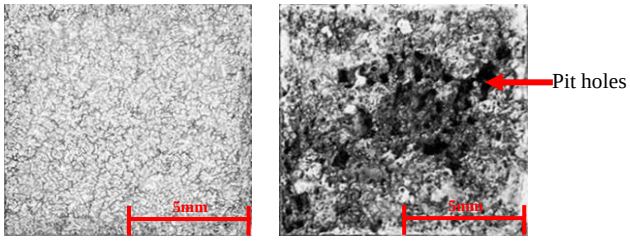

(a) (b)

Fig. 4. Surface appearance for anodised (a) and corroded sample (b).

Figure 5 and Figure 6 show the image from Otsu's thresholding and multilevel thresholding for samples in Group 1 and Group 2. For a binary image of samples 1B, 1C and 1D, the distribution of white region pixels indicate the area of corrosion on the sample. Hence, the high distribution of white region pixels also represents a large corrosion area on the sample. While for the RGB images, the different colour label described yellow (low corrosion), light blue (moderate corrosion) and dark blue (severe corrosion) not only shows the corrosion area on the sample but also shows the corrosion severity.

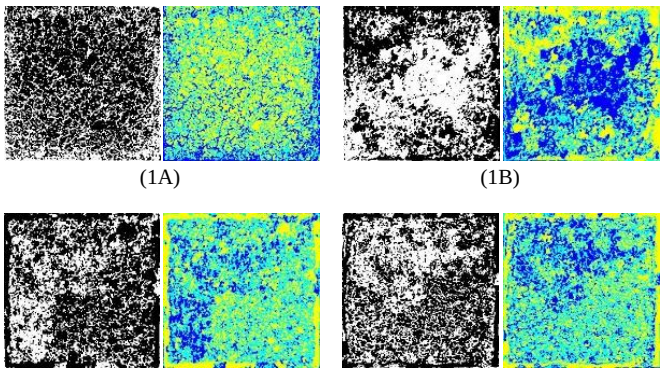

(1A) (1B)

(1C) (1D)

Fig. 5. Binary and RGB images of samples 1A, 1B, 1C and 1D for Group 1.

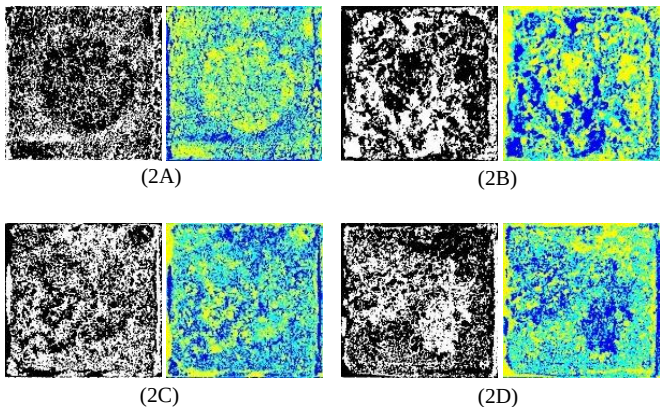

(2A) (2B)

(2C) (2D)

Fig. 6. Binary and RGB images of samples 2A, 2B, 2C and 2D for Group 2.

Pixel Distribution

Figure 7 shows the pixel distribution of the corroded AZ91D magnesium alloy samples in the investigation according to the Zinc Nitrate concentration. For both of the concentrations, it can be seen that the corroded samples pixel's distribution is shifting to the left side and covering a broader range on the low side of the intensity scale compared to the reference sample from each group. This indicates a broader area of corroded surface detected on the sample.

As the corrosion becomes more severe, the pixel's distribution becomes more dominant in the dark regions. Thus, image enhancement by using negative image transformation is then applied to enhance the image's white details [18]. Hence the label of the white region as a corroded surface and the black region as a non-corroded surface.

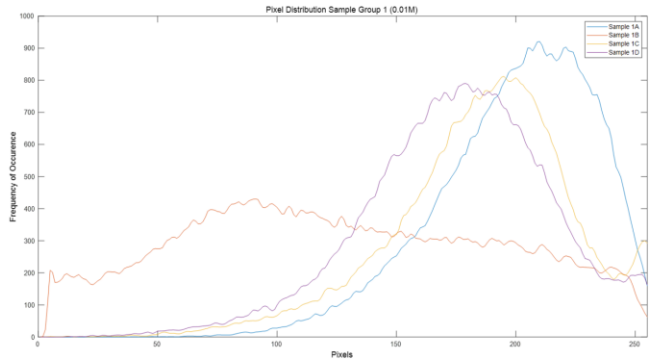

(a)

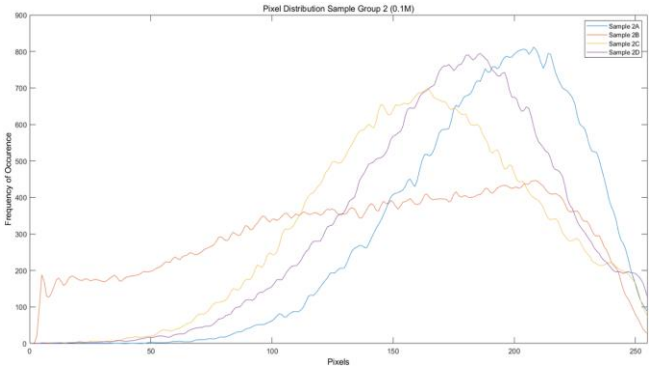

(b)

Fig. 7. Pixel distributions of samples in the investigation according to 0.01M (a) and 0.1M (b) of Zinc Nitrate electrolyte concentration.

Table 3 consists of each sample's corrosion severity in pixel numbers and their corrosion rate, R in millimetres per year. The total corroded pixel (TCP) for the moderate and severe corrosion category is generally

higher than the entire corroded pixel (TCP) for the low corrosion category.

Table 3. Total Corroded Pixel (TCP) numbers and corrosion rate, R-value.

Sample	Corrosion Severity Category (Pixel number)		Corrosion rate (R)
	Moderate & Severe	***Low***	
1A	42063	30561	N/A
2A	44287	27775	N/A
1B	51279	22427	22.61 mm/year
1C	42642	23406	21.00 mm/year
1D	49241	22719	23.87 mm/year
2B	46888	29805	26.46 mm/year
2C	54227	21397	31.43 mm/year
2D	51967	25308	33.74 mm/year

The correlation between Total Corroded Pixel (TCP) and the corrosion rate, R, can be displayed in a linear correlation graph in Figure 8. The increment of corrosion rate does not increase the pixel number of low corrosion; thus, they are negatively correlated in this case. Meanwhile, in the case of moderate and severe corrosion, the pixel number increases as the corrosion rate increase. This shows that these two variables are positively correlated.

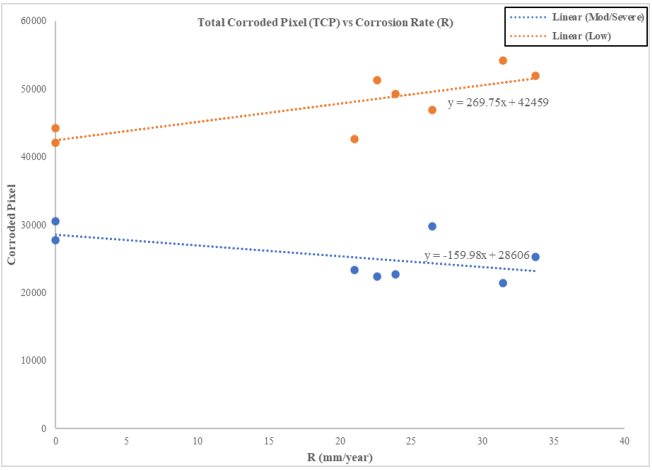

Fig. 8. Linear correlation between Total Corroded Pixel (TCP) and Corrosion Rate, R.

CONCLUSION

This paper analyses the multilevel Otsu thresholding method on anodised and corroded AZ91D Magnesium Alloy samples. The image data set used for this analysis was prepared by acquiring the image of anodised and corroded AZ91D magnesium alloy samples. The corroded area was identified and detected using Otsu's thresholding method. Meanwhile, multilevel Otsu thresholding extracts more corrosion information and categorises it into three categories based on corrosion severity. The corrosion rate data of the samples were also used to correlate with the total corroded pixels. Therefore, with this information, manufacturers can use it to predict the life of a component and manage preventive maintenance activity.

REFERENCES

[1] Y. Chen, Y. Yang, W. Zhang, T. Zhang, and F. Wang, "Influence of second phase on corrosion performance and formation mechanism of PEO coating on AZ91 Mg alloy," *J. Alloys Compd.*, vol. 718, pp. 92–103, 2017, doi: 10.1016/j.jallcom.2017.05.010.

[2] Z. Tang, "A review of corrosion inhibitors for rust preventative fluids," *Current Opinion in Solid State and Materials Science*, vol. 23, no. 4. Elsevier, p. 100759, Aug. 01, 2019, doi: 10.1016/j.cossms.2019.06.003.

[3] P. M. Maurya, "Effect of corrosion on metals and its prevention," vol. 2, no. 2, pp. 1–3, 2022.

[4] M. Z. M. Zamzuri, N. F. W. M. Sidik, M. N. B. Derman, S. Norbahiyah, and M. Mat Salleh, "Improvement of Corrosion Resistance of Az91D Magnesium Alloy By Lanthanum-Based Conversion Coating," *J. Ind. Technol.*, vol. 21, no. 1, pp. 53–61, 2013, doi: 10.21908/jit.2013.6.

[5] W. Khalfaoui, E. Valerio, J. E. Masse, and M. Autric, "Excimer laser treatment of ZE41 magnesium alloy for corrosion resistance and microhardness improvement," *Opt. Lasers Eng.*, vol. 48, no. 9, pp. 926–931, 2010, doi: 10.1016/j.optlaseng.2010.03.009.

[6] Y. Zhang, C. Yan, F. Wang, H. Lou, and C. Cao, "Study on the environmentally friendly anodizing of AZ91D magnesium alloy," *Surf. Coatings Technol.*, vol. 161, no. 1, pp. 36–43, Nov. 2002, doi: 10.1016/S0257-8972(02)00342-0.

[7] N. F. W. M. Sidik, M. Z. M. Zamzuri, M. Mat Salleh, and K. A. Ismail, "Effect of NaVO3 concentration on corrosion resistance of conversion coating on AZ91D magnesium alloy," in *Advanced Materials Research*, 2012, vol. 576, pp. 438–441, doi: 10.4028/www.scientific.net/AMR.576.438.

[8] "Standard Guide for Examination and Evaluation of Pitting Corrosion," *Annual Book of ASTM Standards*, vol. 94, no. Reapproved 2018. pp. 1–8, 1999, doi: 10.1520/G0046-94R18.2.

[9] C. S. Brossia, "Electrical resistance techniques," in *Techniques for Corrosion Monitoring*, Woodhead Publishing, 2020, pp. 267–284.

[10] Y. Yan, "Tribology and tribo-corrosion testing and analysis of metallic biomaterials," in *Metals for Biomedical Devices*, Woodhead Publishing, 2010, pp. 178–201.

[11] D. Itzhak, I. Dinstein, and T. Zilberberg, "Pitting corrosion evaluation by computer image processing," *Corros. Sci.*, vol. 21, no. 1, pp. 17–22, 1981, doi: 10.1016/0010-938X(81)90059-7.

[12] X. Xu, Y. Wang, J. Wu, and Y. Wang, "Intelligent corrosion detection and rating based on faster region-based convolutional neural network," *2020 Glob. Reliab. Progn. Heal. Manag. PHM-Shanghai 2020*, 2020, doi: 10.1109/PHM-

Shanghai49105.2020.9281005.

[13] N. D. Hoang, "Image Processing-Based Pitting Corrosion Detection Using Metaheuristic Optimized Multilevel Image Thresholding and Machine-Learning Approaches," *Math. Probl. Eng.*, vol. 2020, pp. 1–19, 2020, doi: 10.1155/2020/6765274.

[14] A. K. Aijazi, L. Malaterre, M. L. Tazir, L. Trassoudaine, and P. Checchin, "Detecting and Analyzing Corrosion Spots on the Hull of Large Marine Vessels Using Colored 3D Lidar Point Clouds," *ISPRS Ann. Photogramm. Remote Sens. Spat. Inf. Sci.*, vol. III–3, no. July, pp. 153–160, 2016, doi: 10.5194/isprsannals-iii-3-153-2016.

[15] L. Liu, E. Tan, Z. Q. Cai, X. J. Yin, and Y. Zhen, "CNN-based automatic coating inspection system," *Adv. Sci. Technol. Eng. Syst.*, vol. 3, no. 6, pp. 469–478, 2018, doi: 10.25046/aj030655.

[16] B. T. Bastian, J. N, S. K. Ranjith, and C. V. Jiji, "Visual inspection and characterization of external corrosion in pipelines using deep neural network," *NDT E Int.*, vol. 107, no. April, p. 102134, 2019, doi: 10.1016/j.ndteint.2019.102134.

[17] S. Ghanta, T. Karp, and S. Lee, "Wavelet domain detection of rust in steel bridge images," *ICASSP, IEEE Int. Conf. Acoust. Speech Signal Process. - Proc.*, pp. 1033–1036, 2011, DOI: 10.1109/ICASSP.2011.5946583.

[18] R. E. W. Rafael C. Gonzalez, *Digital Image Processing*, Third. Prentice-Hall, Inc.Division of Simon and Schuster One Lake Street Upper Saddle River, NJUnited States, 2006.